First-Principle Study of the Intercalation Process in the $Li_xV_2O_5$ System

Xavier Rocquefelte,* Florent Boucher, Pascal Gressier, and Guy Ouvrard

Institut des Matériaux Jean Rouxel, UMR CNRS 6502, Ecole Polytechnique de l'Université de Nantes BP 32229, 44322 Nantes Cedex 3, France

Received July 4, 2002. Revised Manuscript Received December 5, 2002

A theoretical study of the lithium intercalated $Li_xV_2O_5$ system has been performed using a dual approach, based on ab initio calculations and experimental data. Two main aspects have been investigated: the atomic structure of each phase and the voltage of a lithium battery with a positive electrode made of $Li_xV_2O_5$. This approach leads to proposal of the full atomic arrangement for the different phases obtained during the reaction. Particularly, a structural arrangement is proposed for the debated ω-$Li_3V_2O_5$ phase, based on a full simulation of its X-ray powder diagram. For the first time, an antiferromagnetic ordering is envisioned for ζ-$Li_2V_2O_5$. Finally, a very good simulation of the experimental open circuit voltage (OCV) curve of the battery, from $x = 0$ to $x = 3$, is obtained when the magnetic interactions are considered.

Introduction

During the past few years, an increasing number of studies have been devoted to the first-principle prediction of the electrochemical potential. The efficiency of such an approach was first demonstrated by Aydinol et al. in 1997 for model compounds.[1] Then, some realistic systems have been considered ($Li_{1-x}NiO_2$,[2] $Li_{1-x}CoO_2$,[3] and $Li_xMn_2O_4$[4]) through the calculation of their intercalation voltage, phase stability, or magnetic properties. However, very few studies have been done on realistic systems for which only partial experimental data were available (cell parameters, interatomic distances). Particularly, the case of nontopotactic reactions which induce drastic changes of the host structure is often not considered through first-principle calculations. In this case, the major problem is that no simple relation can be found between the starting structure and the intercalated one. For that reason, it is really difficult to study such a reaction without taking into account the experimental data and just by doing DFT calculations, with only the initial structure as an input variable.

In this study we have considered a lithium-metal battery, where the negative electrode is made of metallic lithium. In a first approximation, this electrode can be considered as not modified during the battery cycling. On the contrary, in the positive electrode, the intercalation compound undergoes redox and/or structural modifications. These changes appear in the open circuit voltage (OCV) curve obtained in the thermodynamic equilibrium conditions. From an industrial point of view, it is of major interest to be able to maintain and control the voltage to a given value of functioning. Then, the understanding of the OCV variations is a crucial aspect. In some cases, such an analysis is made difficult by the loss of cristallinity of the positive electrode upon the lithium intercalation. In this context, we propose an approach coupling experimental data and theoretical methods. Recently, we have successfully applied this approach to the case of lithium intercalation in MoS_2. From structural hypotheses, we proposed an optimized structure for $LiMoS_2$ that is in good agreement with experimental data: simulated X-ray diffraction pattern, bond distances, and cell parameters.[5]

In the present paper we will show that such a dual approach can lead to structural predictions in really good agreement with experimental data in the case of V_2O_5. Moreover, the calculations provide the total energy of the system and allow a simulation of the OCV curve.

We have chosen to study the intercalation reaction in the $Li_xV_2O_5$ system from $x = 0$ to $x = 3$ for many reasons. First of all, several phase transitions occur during the lithium intercalation leading to large changes in the OCV curve.[6] Because of the structural changes the compound loses its cristallinity upon lithium intercalation. Thus, even though a lot of various experimental data are available, the structures of many intercalated phases are not accurately known.

Experimental and Theoretical Backgrounds

The electrochemical behavior of α- and γ'-V_2O_5 is shown in the upper part of the Figure 1. These two

* To whom correspondence should be addressed. Tel: (33) 2 40 37 39 39. Fax: (33) 2 40 37 39 95. E-mail: Xavier.Rocquefelte@cnrs-imn.fr.

(1) Aydinol, M. K.; Kohan, A. F.; Ceder, G. *Phys. Rev. B* **1997**, *56*, 1354−1365.

(2) Arroyo y de Dompablo, M. E.; Marianetti, C.; Van der Ven, A.; Ceder, G. Cationic Ordering in Layered Li_xNiO_2 Compounds in Rechargeable Lithium Batteries. In *Proceedings (Electrochemical Society)*; Abraham, K. M., Takeuchi, E. S., Doyle, M., Eds.; Pennington, NJ, 2000.

(3) Van der Ven, A.; Aydinol, M. K.; Ceder, G.; Kresse, G.; Hafner, J. *Phys. Rev. B* **1998**, *58*, 2975−2987.

(4) Mishra, S. K.; Ceder, G.; *Phys. Rev. B* **1999**, 59, 6120−6130.

(5) Rocquefelte, X.; Boucher, F.; Gressier, P.; Ouvrard, G.; Blaha, P.; Schwarz, K. *Phys. Rev. B* 2000, *62*, 2397−2400.

(6) Delmas, C.; Cognac-Auradou, H.; Cocciantelli, J. M.; Ménétrier, M.; Doumerc, J. P. *Solid State Ionics* **1994**, *69*, 257−264.

10.1021/cm021254h CCC: $25.00
Published on Web 04/11/2003

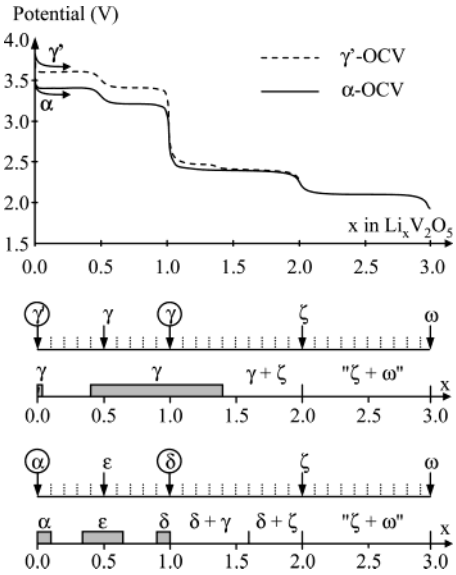

Figure 1. Open circuit voltage (OCV) starting from α and γ'-V_2O_5 and related phase transitions. Grey zones correspond to solid solution domains. The different compositions of the studied phases are indicated by arrows.

curves were deduced from various published galvanostatic intermittent discharge curves of Li/V_2O_5 cell.[6,7] We have considered the data closer to the thermodynamic equilibrium conditions. We use the following notation: α-OCV and γ'-OCV for the OCV starting from α- and γ'-V_2O_5, respectively. The corresponding phase transitions that occur during α-OCV and γ'-OCV are given in the lower part of Figure 1. The α-OCV curve can be viewed as made of four plateaus, each one corresponding to a two−phase process. In this approximation, only 5 limit phases have to be considered and have a physical meaning: α-V_2O_5, ϵ-$Li_{0.5}V_2O_5$, δ-LiV_2O_5, ζ-$Li_2V_2O_5$, and ω-$Li_3V_2O_5$. Electrochemical lithium deintercalation from ζ-$Li_2V_2O_5$ leads to a new phase γ'-V_2O_5, from which a slightly different OCV curve is obtained (Figure 1, upper part, dashed line). The γ'-OCV curve is composed of five plateaus. Neglecting the small voltage drop at $x \approx 1.2$, three other phases must be taken into account: γ'-V_2O_5, γ-$Li_{0.5}V_2O_5$, and γ-LiV_2O_5. Among these eight phases, four accurately determined X-ray structures are available and will be described later. The four others are not precisely known. This lack of experimental information led us to use the geometry optimization (cell parameters and atomic positions) of structural hypotheses based on available experimental data.

A few years ago a theoretical study was performed on this system by Braithwaite et al., in a topotactic approach.[8,9] They have simulated the electrochemical behavior of $Li_xV_2O_5$ from $x = 0$ to $x = 2$, using plane wave calculations based on density functional theory. Due to the topotactic hypothesis, all the so-obtained structures have a more or less distorted α-type structure. The puckering of the V_2O_5 layer for the ϵ phase is well reproduced. However, the experimentally observed b/2 translation every other slab in the δ phase was not found by the calculations. Furthermore, no γ phase is predicted for $x > 1$. This study illustrates the difficulty of simulating the electrochemical behavior without taking into account the experimental results.

This paper is divided into two main parts: a structural part and an electrochemical part. We have considered two OCV curves of $Li_xV_2O_5$ ($0 \leq x \leq 3$), respectively, starting from α-V_2O_5 and γ'-V_2O_5.

Computational Approach

Band Structure Calculation. Our calculations are based on density functional theory and we use the PW91[10,11] generalized gradient approximation (GGA) for the exchange and correlation correction. The electronic structures are obtained at 0 K in using the VASP program.[12,13,14] The eigenstates are expanded in terms of plane waves. Only the eigenstates of valence electrons are taken into account in this method, and pseudopotentials are used to reproduce the effect of the core shell on the valence electrons. The completeness of the basis set is controlled by an energy cutoff defining the number of plane waves included in the basis. The use of ultrasoft pseudopotentials[15,16] allows lowering of the energy cutoff, thus reducing the size of the calculation. The pseudopotentials used in the following calculations correspond to the atomic reference configuration $3p^6$-$4s^13d^4$ for V, $2s^22p^4$ for O, and $2s^12p^0$ for Li. After several tests of energy convergence based on the geometry optimization of lithiated and nonlithiated phases, an energy cutoff of 600 eV is used. The integration into the first Brillouin zone has been performed using 32 k-points for geometry optimization. Then 256 k-points have been considered in order to check the atomic force convergence and to calculate the total energy. The full geometry optimization (cell parameters and atomic positions) is performed using a conjugate−gradient algorithm[14] minimizing the total energy. The structure convergence is controlled by a cutoff condition that in our case consists of stopping the calculation if atomic forces are smaller than 3×10^{-2} eV/Å per atom and if cell stresses lead to energy changes smaller than 10^{-2} eV per unit cell.

Mean Voltage Calculation. The equilibrium voltage between the negative and the positive electrode is defined as the difference of the Li chemical potential between the two electrodes:[17,18]

(7) Cocciantelli, J. M.; Ménétrier, M.; Delmas, C.; Doumerc, J. P.; Pouchard, M.; Hagenmuller, P. *Solid State Ionics* **1992**, *50*, 99−105.
(8) Braithwaite, J. S.; Catlow, C. R. A.; Gale, J. D.; Harding, J. H. *Chem. Mater.* **1999**, *11*, 1990−1998.
(9) Braithwaite, J. S.; Catlow, C. R. A.; Gale, J. D.; Harding, J. H.; Ngoepe, P. E. *J. Mater. Chem.* **2000**, *10*, 239−240.
(10) Perdew, J. P. Vol. 11 in *Electronic Structure of Solids 91*; Ziesche, P., Eschrig, H., Eds.; Akademie Verlag: Berlin, 1991.
(11) Perdew, J. P.; Chevary, J. A.; Vosko, S. H.; Jackson, K. A.; Pederson, M. R.; Singh, D. J.; Fiolhais, C. *Phys. Rev. B* **1992**, *46*, 6671−6687.
(12) Kresse, G.; Hafner, J. *Phys. Rev. B* **1993**, *47*, 558−561.
(13) Kresse, G.; Furthmüller, J. *Comput. Mater. Sci.* **1996**, *6*, 15−50.
(14) Kresse, G.; Furthmüller, J. *Phys. Rev. B* **1996**, *54*, 11169−11186.
(15) Vanderbilt, D. *Phys. Rev. B* **1990**, *41*, 7892−7895.
(16) Kresse, G.; Hafner, J. *J. Phys.: Condens. Matter* **1994**, *6*, 8245−8257.
(17) McKinnon, W. R. Insertion electrodes I: Atomic and electronic structure of the hosts and their insertion compounds; *In Solid State Electrochemistry*; Cambridge University Press: Cambridge, 1995; Ch. 7.
(18) Armand, M. B. *Intercalation electrodes*, *Proceedings of a NATO Symposium on Materials for Advanced Batteries*; Plenum: New York, 1980.

$$V(x) = \frac{\mu_{\mathrm{Li}}^{\mathrm{positive}}(x) - \mu_{\mathrm{Li}}^{\mathrm{negative}}}{zF}$$

where F is the Faraday constant and z is the charge (in electrons) transported by lithium in the electrolyte. Here the ionic conduction is ensured by Li cation, thus $z = 1$. Using several approximations,[1] we can calculate the mean potential based on total energy calculations. The different approximations are summarized as follows. (1) The displaced charge is only due to Li^+ and the electrons. As a consequence of the two-phase process approximation, an intermediate composition will correspond to the coexistence of two limit phases in an appropriate amount. In that case, no configurational Li disorder has to be taken into account. (2) The variation in the Gibbs free energy (ΔG) is approximated by the change (ΔE) in the internal energy at 0 K by neglecting the volume ($P\Delta V$) and entropic ($T\Delta S$) variations ($\Delta G = \Delta E + P\Delta V - T\Delta S$).

In this frame, the determination of an average intercalation voltage requires only three total energy calculations: the metallic lithium one in the body-centered-cubic structure and the two limit phases for the intercalation compound. We use the following equation:[1]

$$\bar{V}(x_1, x_2) = \frac{-[E_{\mathrm{Li}_{x_2}\mathrm{V_2O_5}} - E_{\mathrm{Li}_{x_1}\mathrm{V_2O_5}} - (x_2 - x_1)E_{\mathrm{Li}}]}{(x_2 - x_1)}$$

where E is a total internal energy and x_1 and x_2 are the two limit compositions. Because we are not in a topotactic case and in order to get most accurate energies, a particular attention has been paid to the structural hypotheses based on experimental data and all atoms are allowed to relax.

Results and Discussion

Pseudopotential Validation. Before starting to optimize the structure of the not well-known phases, it was necessary to check the quality of the pseudopotentials. First, we fully optimized the structures of the known phases (α, δ, γ', and γ) and checked the agreement between experimental data and calculations. Our results are summarized for α-V_2O_5 and δ-LiV_2O_5 in Tables 1 and 2, respectively. For both compounds, the known crystallographic structures[19, 21] have been considered as input in the calculation.

The pristine phase consists of the stacking of weakly interacting V_2O_5 layers along the c axis (Figure 2). As shown in Table 1, the optimization leads to cell parameters and interatomic distances in good agreement with the experimental data.[19] The optimized cell parameters are approximately 1% larger than experimentally found except for the stacking parameter (of about 2.5%). In fact, interlayers interaction are small (van der Waals type) and are not completely taken into account in such GGA calculations. If we now have a look at the interatomic distances in α-V_2O_5, it can be noticed that the VO_5 square pyramid is correctly reproduced by the calculation, with a short apical double bond (optimized vanadyl bond: 1.61 Å) and 4 longer V−O bonds (average optimized value: 1.91 Å). The sixth V−O distance (pseudo-octahedral coordination) is slightly overestimated. This clearly demonstrates that the error on the stacking parameter comes exclusively from an incomplete description of the interlayer interaction.

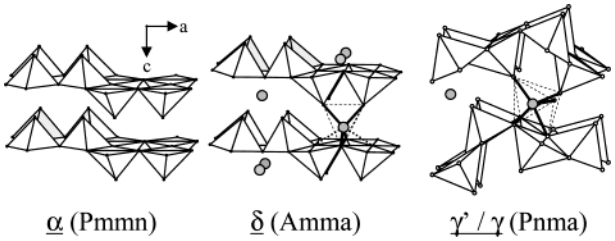

Figure 2. Schematic representation of the experimentally well-determined $Li_xV_2O_5$ structures.

Table 1. Comparison of Theoretical and Experimental[19] Cell Parameters and Interatomic Distances in α-V_2O_5

	exp. (Å)	calc. (Å)	diff. (%)
a	11.51	11.69	1.6
b	3.56	3.59	0.7
c	4.37	4.48	2.5
V=O (×1)	1.59	1.61	1.5
V−O (×4)	1.89 [1.78:2.02]	1.91 [1.80:2.05]	1.1
V···O (×1)	2.79	2.87	3.0

Table 2. Comparison of Theoretical and Experimental[21] Cell Parameters and Interatomic Distances in δ-LiV_2O_5

	exp. (Å)	calc. (Å)	diff. (%)
a	11.24	11.35	1.0
b	3.60	3.63	0.8
c	9.91	9.97	0.7
V=O (×1)	1.61	1.62	0.7
V−O (×4)	1.91 [1.87:1.96]	1.93 [1.86:2.01]	1.0
Li−O (×4)	2.07 [2.04:2.10]	2.09 [2.02:2.15]	1.0
Li−O (×2)	2.38	2.45	2.9

The δ-LiV_2O_5 structure is based on slightly puckered α-type layers (Figure 2). The packing differs from the α one by a $b/2$ translation every other slab and, as a consequence the c parameter is doubled.[6] The V coordination is thus modified from pseudo-octahedral (in α) to square pyramid (in δ). As for the α phase, the optimized cell parameters and V−O bonds of the δ-LiV_2O_5 phase (Table 2) are in good agreement with experimental data.[21] Li coordination is a bicapped tetrahedron according to Brown calculations:[22] Lithium valency is equal to 0.77 with the tetrahedron coordination and 0.91 with the complete bicapped tetrahedron coordination ($r_0 = 1.466$ Å and $B = 0.37$ Å). Li−O bond distances, presented in Figure 2, are well reproduced. A similar agreement is found for γ'-V_2O_5 and γ-LiV_2O_5.[23,24]

From a structural point of view, the oxygen, vanadium, and lithium pseudopotentials accurately repro-

(19) Enjalbert, R.; Galy, J. *Acta Crystallogr. C* **1986**, *42*, 1467−1469.
(20) Cognac-Auradou, H. *Les phases ω-$Li_xV_2O_5$, nouveaux matériaux d'électrode pour batteries au lithium. Caractérisation structurale et électrochimique*. Ph.D. Thesis, Bordeaux, 1993.
(21) Cava, R. J.; Santoro, A.; Murphy, D. W.; Zahurak, S. M.; Fleming, R. M.; Marsh, P.; Roth, R. S. *J. Solid State Chem.* **1986**, *65*, 63−71.
(22) Brown, I. D.; Altermatt, D. *Acta Crystallogr. B* **1985**, *41*, 244−247.
(23) Cocciantelli, J. M.; Gravereau, P.; Doumerc, J. P.; Pouchard, M.; Hagenmuller, P. *J. Solid State Chem.* **1991**, *93*, 497−502.
(24) Galy, J.; Darriet, J.; Hagenmuller, P. *Rev. Chim. Min.* **1971**, *8*, 509−522.

duce the bonding in these well-known compounds. Therefore, these pseudopotentials have been kept for the calculations on the other phases.

Structure Prediction. As mentioned in the computational part, we optimized the structure of all the limit phases in order to obtain the best possible total internal energies. Structural hypotheses have been based on available experimental data. In these cases, the poor quality of XRD data and some NMR results have only been able to conclude to a maintaining of the general structural frame for ϵ and ζ phases, and a transition to a pseudo rocksalt structure for ω. Full geometry optimization was performed in P1 symmetry in order to allow a maximum degree of freedom for the atomic motions and cell distortion. A random displacement has been previously applied to the atoms. Discrimination between different hypotheses was done using total energy criterion.

Whereas during the first discharge starting from α-V_2O_5, major structural changes occur, γ-type structure is kept during the first discharge starting from γ'-V_2O_5.[7] In the following they are treated separately.

Study of the Phases Formed during α*-OCV.* Among the five phases which are necessary to correctly describe the α-OCV curve, two of them (α, δ) have already been discussed. We will present the results of the structural optimization for the three other phases (ϵ, ζ, ω).

(*1*) ϵ-$Li_{0.5}V_2O_5$. It has been clearly established that the ϵ phase is related to the α-type arrangement with a small puckering of the layers. Various studies tried to define the location of the lithium atom in the empty sites of the puckered V_2O_5 layers. [6,25,26] They led to significantly different results, and therefore a complete description of the ϵ phase is not available. To obtain information in this matter from DFT calculations, we started from the structural hypothesis of Coccianteli et al., who synthesized the ϵ phase electrochemically.[27] Because of the very small electrochemical potential variations, only the $x = 0.5$ composition has been considered.

For the calculations, a Li occupancy of every other site along [100] and [010] directions has been considered. This leads to a doubling of *b* parameter and a reducing of space group symmetry from *Pmmn* to $P2_1/m$. The symmetry was allowed to vary but the optimized structure keeps the $P2_1/m$ symmetry. Starting from nonpuckered layers (Figure 3a) and Li atoms at the center of bicapped trigonal prismatic sites (Figure 3c), the optimization leads to a significantly puckered structure (Figure 3b). The origin of the puckering can be explained by the distortion of the Li site (Figure 3d). As it is frequently observed, lithium tends to have a low coordination due to its high polarizing power. Here, the Li sits near one triangular face of bicapped trigonal prism (Figure 3d). Reasonable cation−oxygen distances are found in the optimized structure (Figure 3, right). A very good agreement is obtained with the experimental values of *a* and *b* parameters (Table 3).

(*2*) ζ-$Li_2V_2O_5$. From $x = 0$ to $x \approx 1$, α to ϵ and ϵ to δ phase transitions are reversible.[6] These three structures

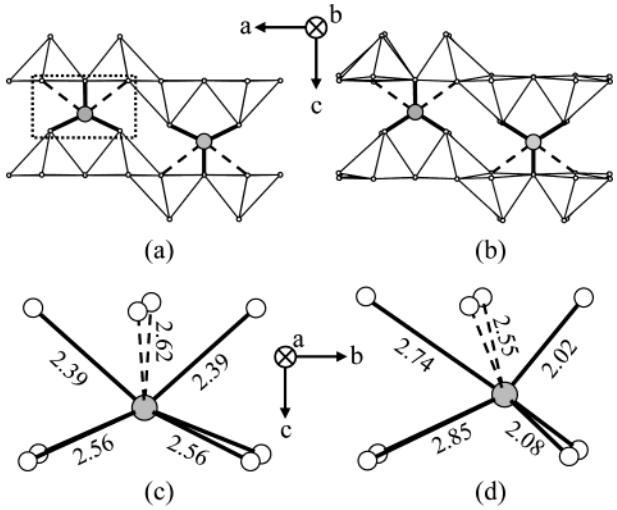

Figure 3. View of the initial (a) and optimized (b) ϵ-$Li_{0.5}V_2O_5$ structures and corresponding lithium environment and Li−O distances (c and d).

differ mainly in the Li coordination. Beyond $x \approx 1$, an irreversible phase transition occurs leading to the γ type structure, shown in Figure 2. The arrangement of the VO_5 square pyramids is largely different from that encountered in α-type. They still share edges and corners, but, as can be seen in Figure 2, their arrangement along the *a* axis is changed from "up−up−down−down" to " up−down−up−down", where up and down stand for the vanadyl bond orientation. Moreover, a strong modification of the basal oxygen position occurs, which can be described as a zigzag shape when projected along the *b* axis.

From $x = 1$ to $x = 2$, two different phase transitions are observed in the lower part of Figure 1: the first one between δ and γ phases and the second one between γ and ζ phases.[7] The ζ structure has been suggested to be not very different from the γ one and the voltage variation along these two transitions is approximately zero. Therefore, we have considered only one phase transition between δ-LiV_2O_5 and ζ-$Li_2V_2O_5$. The structural hypothesis for ζ-$Li_2V_2O_5$ was constructed from the γ-$Li_1V_2O_5$ atomic positions[24] with the ζ phase experimental cell parameters.[7] In this structure, the first Li atom fully occupies the octahedral site. It was suggested by Coccianteli et al. that the second Li sits in one of the available tetrahedral sites, but, for electrostatic reasons, the occupancy of this tetrahedral site could not exceed 0.4.[28] Such an hypothesis cannot explain the structure of the phase in which the Li/V_2O_5 ratio is 2. Therefore, we decided to start the structural optimization with a fully occupied tetrahedral site (Figure 4a and c).

The relaxed structure keeps a γ-type arrangement (Figure 4b) and the space group is unchanged (*Pnma*). A slightly distorted octahedral site is found for the first Li atom (Figure 4d) with Li−O distances in agreement with the ones observed in γ-$Li_1V_2O_5$. After the optimization, the second lithium atom leaves the approximate center of the tetrahedron and moves toward a triangular face shared by two tetrahedra (Figure 4d). It's coordi-

(25) Galy, J. *J. Solid State Chem.* **1992**, *100*, 229−245.
(26) Rozier, P.; Savariault, J. M.; Galy, J.; Marichal, C.; Hirschinger, J.; Granger, P. *Eur. J. Solid State Inorg. Chem.* **1996**, *33*, 1−13.
(27) Coccianteli, J. M. Caractérisation physico-chimique d'électrodes positives de composition $Li_xV_2O_5$; Ph.D. Thesis, Bordeaux, 1990.
(28) Coccianteli, J. M.; Suh, K. S.; Sénégas, J.; Doumerc, J. P.; Soubeyroux, J. L.; Pouchard, M.; Hagenmuller, P. *J. Phys. Chem. Solids* **1992**, *53*, 51−55.

Table 3. Comparison of Theoretical and Experimental Cell Parameters in ϵ-$Li_{0.5}V_2O_5$,[27] ζ-$Li_2V_2O_5$,[7] and ω-$Li_3V_2O_5$[29]

	ϵ-$Li_{0.5}V_2O_5$			ζ-$Li_2V_2O_5$			ω-$Li_3V_2O_5$		
	exp. (Å)	calc. (Å)	diff. (%)	exp. (Å)	calc. (Å)	diff. (%)	exp. (Å)	calc. (Å)	diff. (%)
A	11.41	11.42	0.0	9.80	9.90	1.0	9.23	9.21	−0.2
B	7.13	7.17	0.6	3.60	3.73	3.5	9.23	9.13	−1.1
C	4.52	4.72	4.6	10.24	10.48	2.3	4.11	3.95	−3.9

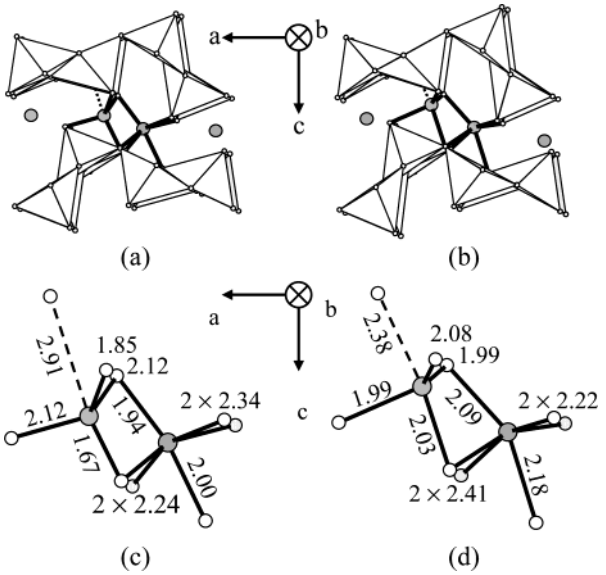

Figure 4. View of the initial (a) and optimized (b) ζ-$Li_2V_2O_5$ structures and corresponding lithium environments and Li−O distances (c and d).

nence is more accurately described as a trigonal bipyramidal site. This situation corresponds to either a stable structure or an average one with half-occupancy of two adjacent tetrahedral sites. For this reason, we started a new optimization from a structural hypothesis based on this latter solution. However, this structure is not stable: the two lithium atoms move again from the center of the tetrahedra to the trigonal bipyramidal sites. This coordination is somewhat unusual but the Li−O distances are reasonable according to Brown calculation[22] (lithium valency is equal to 1.00 using r_0 = 1.466 Å and B = 0.37 Å) and it seems to be the only one which minimizes the electrostatic Li−V repulsions.

(*3*) *ω-Li$_3$V$_2$O$_5$.* The structure of ω-$Li_3V_2O_5$ obtained at the end of the first discharge (room temperature) is claimed to be based on the rocksalt type with a superstructure due to a lithium/vanadium ordering. This superstructure has been indexed, from electron diffraction experiments, with a tetragonal cell: a = 9.23 Å, c = 4.11 Å, Z = 4.[20,29] The main question in this structure is the respective arrangement between Li and V in the available octahedral sites. Figure 5a is a schematic representation of a projection of the NaCl unit cell where only metal sites are shown. Metal sites at z = 0 and 0.5 are represented by large and small circles, respectively. To allow a distortion of this arrangement, a quadratic cell (Figure 5c) has been considered from a 3a × 3a cubic supercell (Figure 5b). This type of representation will be used to describe the different models proposed for the Li/V ordering. In fact, so many Li/V arrangements are compatible with the proposed

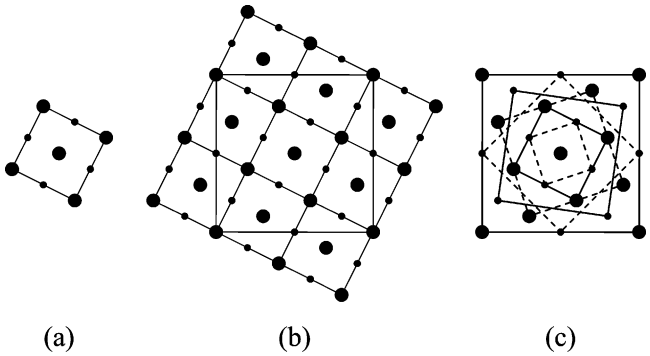

Figure 5. Schematic illustration of the ω-$Li_3V_2O_5$ cell construction: simple rock-salt unit cell (a), 3a × 3a rock-salt supercell showing the ω unit cell (b) and ω unit cell (c). Only cationic (Li/V) sites are represented. Sites at z = 0 and 0.5 are represented by large and small circles, respectively. Sites related by the 4-fold axis are connected by solid (z = 0) and dotted (z = 0.5) lines.

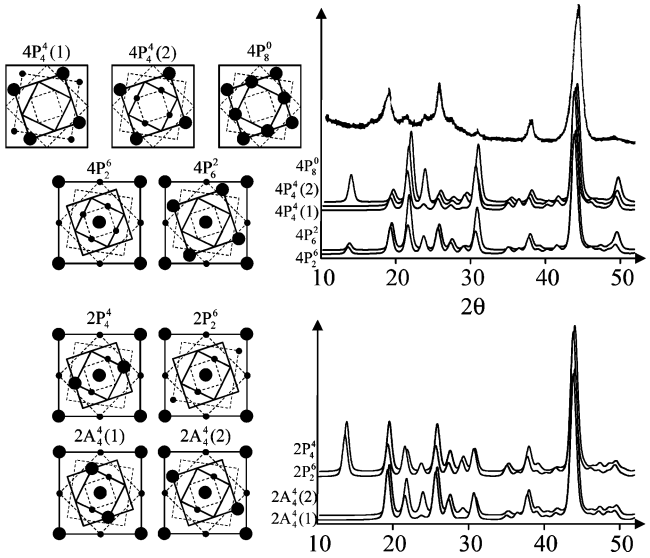

Figure 6. Left: schematic illustration of the proposed vanadium arrangements for ω-$Li_3V_2O_5$ having 4-fold symmetry (4P) or 2-fold symmetry (2P and 2A). Right: corresponding X-ray diagram simulations. On top, the experimental X-ray diagram is given.

unit cell that a first step of this study consisted of reducing the investigation field using two main criteria: the comparison of simulated and experimental X-ray diagram and the total energy of the optimized system. Before starting any optimization, we first envisioned the ordered structures with the highest symmetry compatible with the unit cell. The upper part of Figure 6 gives an illustration of the five structures which have a 4-fold axis (*P*4/*m* space group). For clarity, only vanadium atoms are represented. To visualize the 4-fold symmetry, squares have been drawn to connect symmetry-related positions with solid and dotted lines for the z = 0 and z = 0.5 planes, respectively. Special notation is used to label the different arrangements: for

(29) Delmas, C.; Brèthes, S.; Ménétrier, M. *J. Power Sources* **1991**, *34*, 113−118.

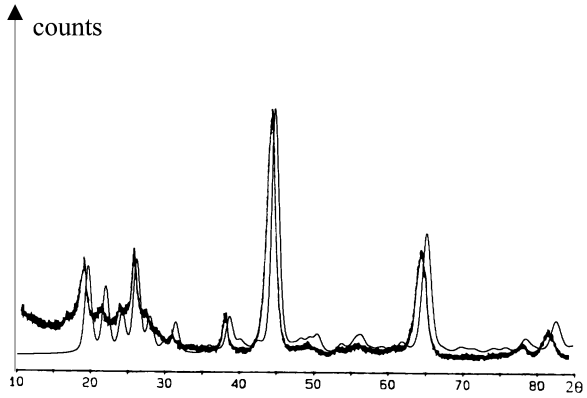

Figure 7. Comparison of the experimental X-ray diagram of ω-$Li_3V_2O_5$ with the simulation corresponding to the more stable ordered structure: $2A_4^4(2)$.

Table 4. Comparison of the Total Energy Per Formula Units (meV/f.u.) of Different V Arrangements for ω-$Li_3V_2O_5$ (See Figure 6 for the Symbols); the More Stable Structure Is Taken as a Reference

tetragonal		monoclinic	
$4P_4^4(1)$	555	$2A_4^4$	224
$4P_4^4(2)$	364	$2A_4^4$	0
$4P_8^0$	318		
$4P_6^2$	322		
$4P_6^2$	192		

example $4P_6^2$ means that there is a 4-fold axis, the lattice is primitive, and 6 (2) vanadium atoms are at $z = 0$ (0.5) (if needed an ordering number is added). The corresponding X-ray diffraction diagram simulations for low angle values (from $2\theta = 10°$ to 50°) are given in Figure 6. These diagrams can be compared with the experimental one. The discrimination between them is mainly based on the intensity of diffraction peaks for $10° < 2\theta < 35°$. There is no doubt that the best model corresponds to the $4P_2^6$ structure in relation to relative intensities of the strong and weak peaks. This has been confirmed by total energy calculations after either an optimization of the internal coordinates using the experimental cell parameters, or a full geometry optimization (Table 4). However, some discrepancies remain on the $4P_2^6$ model. To improve the simulations we have considered other orderings with lower symmetries. Analysis of the diffracted intensities of the $4P_2^6$ model shows that at least a pattern with four vanadium atoms in face-centered positions is required for a good simulation. With this restriction, only four different models having the highest Laue symmetry compatible with the choice of the unit cell, i.e., the monoclinic 2/*m*, are possible. They are presented in Figure 6 (bottom) together with the corresponding simulations. The $2P_2^6$ and $2P_4^4$ models give nonsatisfying X-ray diagram simulation. Particularly, an intense peak is found at about $2\theta = 15°$ in disagreement with experimental observations. Hence, these two models were no longer considered. The structures of the two other models were then fully optimized and the total energy calculations show that the most stable structure is obtained from the $2A_4^4(2)$ model (Table 4). In this case, a really good agreement is found between the experimental X-ray diagram and the simulation based on the optimized structure of the $2A_4^4(2)$ model (Figure 7). This allows concluding that the $Li_3V_2O_5$ superstructure can be effectively described in the tetragonal cell proposed by Delmas et al. using the nonconventional monoclinic space group *A*2/*m* (*A*112/*m*, unique axis c). It should be noticed, however, that two problems were encountered during the unit cell optimization procedure. First, a small deviation from 90° was found for the γ angle with only a small effect on the total energy. In the following calculations this angle was constrained to 90°. Second, all the optimized lattice parameters were found ≈2% too small (Table 3) compared to the experimental values. This behavior is peculiar in the series of our calculations. It can be explained by three main differences between ω-$Li_3V_2O_5$ and the other phases: (i) the dimensionality, which is 3D instead of 2D; (ii) the significantly reduced oxidation state of vanadium atoms, which may affect the pseudopotential transferability; and (iii) the increase of the intra-atomic d−d electronic interactions, which is another consequence of this vanadium reduction and may be not properly taken into account by GGA calculations.

Phases Formed from γ'-OCV. During the first discharge starting from γ'-V_2O_5, the structure is not deeply modified. The γ-type (Figure 2), previously described for ζ-$Li_2V_2O_5$, persists all along the Li intercalation up to $x = 2$ (Figure 1 bottom).[7,30] Only a significant evolution of the stacking parameter is observed during the intercalation. If we want to properly describe the OCV curve, we have to consider four γ-type phases with the following compositions: $x = 0$, 0.5, 1, and 2. Three compositions have already been investigated; the only missing one is γ-$Li_{0.5}V_2O_5$. The only available experimental data for this phase are the cell parameters. The structural hypothesis for γ-$Li_{0.5}V_2O_5$ was constructed from the γ-$Li_1V_2O_5$ atomic positions[24] with the γ-$Li_{0.5}V_2O_5$ experimental cell parameters.[7] For the calculations, a Li occupancy of every other octahedral site along [100] and [010] directions has been considered. This leads to a reducing of space group symmetry from *Pnma* to $P2_1/m$. The optimized cell parameters are in good agreement with the experimental ones.

To validate our calculation, we compared the evolution of the optimized and experimental stacking parameters for the different *x* values (Figure 8). A systematic overestimation of cell parameters is observed with a larger error in the case of γ'-V_2O_5 due to small interlayers interactions, as for α-V_2O_5. Nevertheless, it is remarkable that the calculation reproduces the decrease of the stacking parameter for $x = 2$. This is another proof that the lithium is correctly positioned in the proposed ζ-$Li_2V_2O_5$ structure. The decrease of the stacking parameter for $x = 2$ could be due to an efficient minimization of the cationic electrostatic repulsions when the lithium fully occupies the trigonal bipyramidal site. All the so-obtained cell and atomic parameters of the optimized structures are reported in ref 31.

(30) Cocciantelli, J. M.; Doumerc, J. P.; Pouchard, M.; Broussely, M.; Labat, J. *J. Power Sources* **1991**, *34*, 103−111.

(31) **α-V_2O_5**: *Pmmn*; $a = 11.693$ Å, $b = 3.589$ Å, $c = 4.476$ Å; V_1: 0.1016 3/4 0.8895; O_1:0.0679 1/4 0.9917; O_2:0.1041 3/4 0.5303; O_3: 1/4 3/4 0.9935. **ϵ-$Li_{0.5}V_2O_5$**: $P2_1/m$ 1 1; $a = 11.418$ Å, $b = 7.168$ Å, $c = 4.724$ Å, $\alpha = 90.0°$; Li_1: 3/4 0.9432 0.3465; V_1: 0.0996 0.3726 0.0989; V_2: 0.9000 0.1216 0.8845; O_1: 0.9284 0.3724 0.9809; O_2: 0.1087 0.3532 0.4387; O_3: 0.0734 0.1219 0.9703; O_4: 3/4 0.6286 0.0163; O_5: 0.8798 0.0986 0.5457; O_6: 3/4 0.1207 0.0142. **δ-LiV_2O_5**: *Amma*; $a = 11.355$ Å, $b = 3.632$ Å, $c = 9.975$ Å; Li_1: 1/4 0 0.1008; V_1: 0.1010 0 0.7947, O_1: 0.1273 0

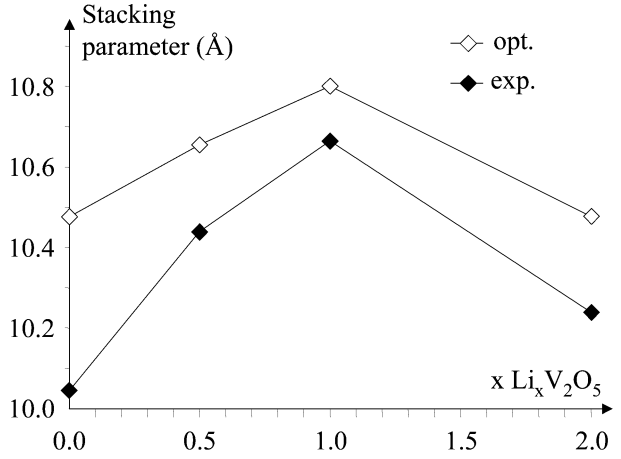

Figure 8. Evolution of the stacking parameter in the γ phases as a function of the Li rate. Black and white diamonds correspond to experimental (exp.) and optimized (opt.) values, respectively.

Magnetic Interaction in V d^1 Phases. In the first step of this study we have been able to propose a structural arrangement for all the phases appearing in the $Li_xV_2O_5$ system. We may use the total energy of these atomic arrangements to simulate the OCV curves. In this approach it appears worthwhile, at least for some phases, to take into account the existence of a magnetic moment on vanadium atoms. To do so, we have performed spin-polarized calculations for γ-LiV_2O_5 and ζ-$Li_2V_2O_5$ compounds. In a periodic approach, a magnetic cell has to be considered. We have tested two different possibilities for γ-LiV_2O_5: the ferromagnetic (F) one, which keeps the full crystallographic symmetry, and an antiferromagnetic (AF) one. In this compound, unlike δ-LiV_2O_5, two kinds of vanadium atoms with different oxidation states (V^{+5} and V^{+4}) are experimentally observed. The AF cell was defined according to experimental data of Isobe et al. It corresponds to an infinite double linear chain with an AF coupling along the chain axis (Figure 9a). In the case of ζ-$Li_2V_2O_5$, no experimental data are available about the possible occurrence of magnetic properties. We have then decided to generalize the AF γ-LiV_2O_5 magnetic structure to the ζ-$Li_2V_2O_5$ one, considering a magnetic moment on every vanadium atom (Figure 9b). For both compounds, a magnetic stabilization appears compared to the nonspin polarized calculations. Also, as shown in Table 5 and in agreement with experimental data and Kanamori-

0.9547; O$_2$: 0.9265 0 0.7579; O$_3$: $^1/_4$ 0 0.7165. **ζ-$Li_2V_2O_5$**: *Pnma*; a = 9.897 Å, b = 3.725 Å, c = 10.478 Å; Li$_1$: 0.1382 $^1/_4$ 0.2295; Li$_2$: 0.1753 $^1/_4$ 0.8250; V$_1$: 0.1263 $^3/_4$ 0.0161; V$_2$: 0.9405 $^3/_4$ 0.3996; O$_1$: 0.2606 $^3/_4$ 0.1409; O$_2$: 0.0181 $^3/_4$ 0.2538; O$_3$: 0.2201 $^3/_4$ 0.8777; O$_4$: 0.0732 $^1/_4$ 0.0304; O$_5$: 0.4426 $^1/_4$ 0.0492. **ω-$Li_3V_2O_5$**: *A* 1 1 2/*m*; a = 9.213 Å, b = 9.133 Å, c = 3.950 Å, γ = 90.0°; Li$_1$: 0.8072 0.3990 0; Li$_2$: 0.3869 0.1948 0; Li$_3$: 0.0923 0.2950 0; V$_1$: 0.7009 0.1139 0; V$_2$: 0 0 0; V$_3$: $^1/_2$ 0 $^1/_2$; O$_1$: 0 0 $^1/_2$; O$_2$: 0.8957 0.1902 0; O$_3$: 0.3025 0.3925 0; O$_4$: 0.8062 0.9205 0; O5:0.6022 0.3049 0; O$_6$: $^1/_2$ 0 0. **γ-V_2O_5**: *Pnma*; a = 10.107 Å, b = 3.599 Å, c = 10.476 Å; V$_1$: 0.1260 $^3/_4$ 0.0162; V$_2$: 0.9293 $^3/_4$ 0.3981; O$_1$: 0.2551 $^3/_4$ 0.1363; O$_2$: 0.0025 $^3/_4$ 0.2619; O$_3$: 0.2116 $^3/_4$ 0.8872; O$_4$: 0.0703 $^1/_4$ 0.0357; O$_5$: 0.4385 $^1/_4$ 0.0437. **γ-$Li_{0.5}V_2O_5$**: $P2_1/m$; a = 9.910 Å, b = 3.636 Å, c = 10.656 Å, β = 90.77°; Li$_1$: 0.3309 $^1/_4$ 0.2727; V$_1$: 0.1264 $^1/_4$ 0.9915; V$_2$: 0.3814 $^3/_4$ 0.4969; V$_3$: 0.0669 $^3/_4$ 0.4013; V$_4$: 0.4332 $^1/_4$ 0.9004; O$_1$: 0.2550 $^1/_4$ 0.8725; O$_2$: 0.2467 $^3/_4$ 0.3702; O$_3$: 0.9957 $^3/_4$ 0.2651; O$_4$: 0.4854 $^3/_4$ 0.2328; O$_5$: 0.2195 $^1/_4$ 0.1193; O$_6$: 0.2956 $^3/_4$ 0.6228; O$_7$: 0.0726 $^3/_4$ 0.9692; O$_8$: 0.4228 $^1/_4$ 0.4531; O$_9$: 0.4382 $^3/_4$ 0.9558; O$_{10}$: 0.0635 $^1/_4$ 0.4567. **γ-$Li_1V_2O_5$**: *Pnma*; a = 9.818 Å, b = 3.625 Å, c = 10.802 Å; Li$_1$: 0.1644 $^1/_4$ 0.2256; V$_1$: 0.1260 $^3/_4$ 0.0022; V$_2$: 0.9384 $^3/_4$ 0.4022; O$_1$: 0.2548 $^3/_4$ 0.1272; O$_2$: 0.0204 $^3/_4$ 0.2694; O$_3$: 0.2189 $^3/_4$ 0.8769; O$_4$: 0.0744 $^1/_4$ 0.0417; O$_5$: 0.4338 $^1/_4$ 0.0440.

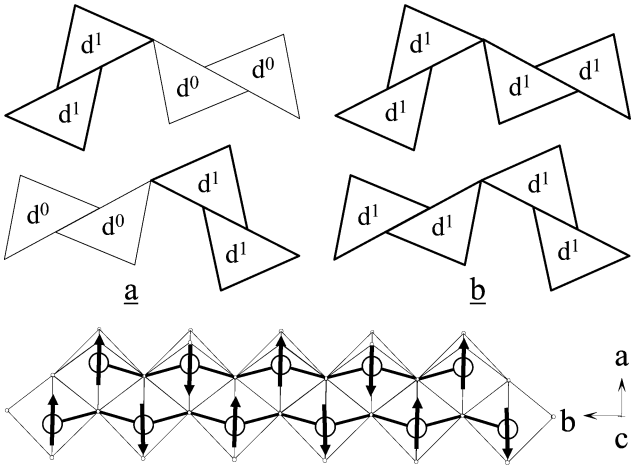

Figure 9. Top: charge ordering in γ-$Li_1V_2O_5$ (a) and in ζ-$Li_2V_2O_5$ (b). Bottom: antiferromagnetic spin ordering along the double linear chains.

Table 5. Cohesive Energy Per Formula Units (eV/f.u.) for the More Stable Optimized Structures of $Li_xV_2O_5$

x Li	0	0.5	1	2	3
α-OCV	−59.089	−61.558	−63.943	−67.862 (AF) −67.468 (NSP)	−71.125
γ-OCV	−58.992	−61.545	−64.097 (AF) −64.071 (F) −63.992 (NSP)	−67.862 (AF) −67.468 (NSP)	

[a] NSP, F, and AF: non-spin polarized, ferromagnetic, and antiferromagnetic calculations, respectively.

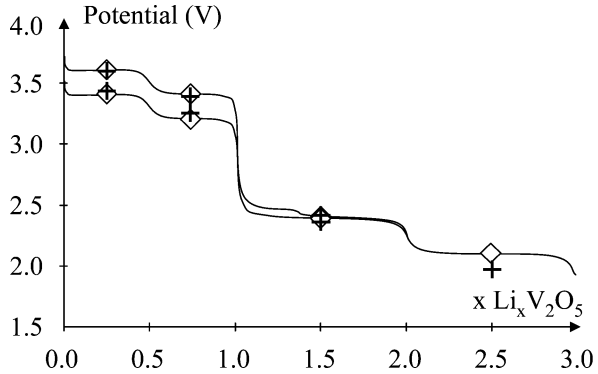

Figure 10. Comparison of experimental (diamonds) and theoretical (crosses) electrochemical mean potentials corresponding to the first discharge starting from α-V_2O_5 and γ'-V_2O_5. A systematic correction of +0.4 V has been applied to the calculated values.

Goodenough rules, the AF ordering is slightly more stable than the F one for the magnetic structure of γ-LiV_2O_5. However, it is apparent that the main part of the stabilization comes from the moment that is created on the vanadium ions and only a smaller contribution comes from the long-range magnetic order. Then, it is justified to do total energy calculations at 0 K for interpretation of room-temperature electrochemical behavior in the paramagnetic domain.

First Discharge Curve Simulation. Now that we know all the atomic structures and their respective total energies, we can estimate the mean voltage for each plateau. Table 5 gathers the total energies corresponding, for each phase, to the most satisfactory optimized structure. As expected, we can notice that the cohesive energy continuously decreases upon the Li insertion. From this cohesive energy, the mean voltage for the

different plateaus has been calculated using the defined above formula. These calculated potentials are represented together with the experimental ones on Figure 10. Considering the remark of Aydinol et al.[1] about an overestimation of 0.4 eV for the Li cohesive energy from DFT methods, we have corrected all the calculated potentials: V_{cor} (eV) = V_{calc} (eV) + 0.4. The results are in a really good agreement with the experimental ones. Furthermore, it clearly appears that taking into account the magnetic properties of ζ-$Li_2V_2O_5$ significantly improves the OCV curve simulation. Without introducing the magnetic exchange, the calculated mean potential at $x = 1.5$ is underestimated by about 0.4 V. A similar effect is observed for γ-LiV_2O_5.

Concluding Remarks

After validating the V, O, and Li pseudopotentials by optimizing the structure of the well-known phases (α and δ), we have defined complete structures for the other intercalated phases (ϵ, ζ, and ω). A very good agreement is obtained with the available experimental data. In the particular case of the ζ-$Li_2V_2O_5$, we obtained a stable structure in which the second lithium atom fully occupies a trigonal bipyramidal site. This unusual coordination seems to be the best way to minimize the cationic electrostatic repulsions. For the ω-$Li_3V_2O_5$ phase, we have been able to accurately simulate the experimental X-ray diagram with a particular Li/V ordering. This allows proposal of a structure with a monoclinic space group $A2/m$.

As for the OCV curve starting from γ'-V_2O_5, we have seen that no important structural changes are observed during the lithium intercalation. The stacking parameter increase up to $x = 1.4$, and a decrease for $x = 2$ is well reproduced by the calculation. The decrease of the stacking parameter in ζ-$Li_2V_2O_5$ must be related to the full occupation of the trigonal bipyramidal site by the second lithium. This last observation reinforces our structural model for ζ-$Li_2V_2O_5$.

Finally, the OCV curves are well reproduced by the calculation if the magnetic properties of γ-LiV_2O_5 and ζ-$Li_2V_2O_5$ are taken into account. The appearance of a magnetic moment on the V ions appears to play a significant role in vanadium oxides in which vanadium atoms have a d^1 electronic configuration. Furthermore, for the first time a magnetic structure is proposed for ζ-$Li_2V_2O_5$.

This study was essentially dedicated to structural determination and electrochemical behavior simulation of $Li_xV_2O_5$. The next step will consist of the understanding of the potential variation origins. In particular, how can we explain the sudden potential decrease for $x = 1$, and why do we observe this phenomenon in both α- and γ'-OCV curves? These fundamental aspects will be discussed in a forthcoming paper.

Acknowledgment. We thank Georg Kresse at Technical University Vienna for kindly giving us permission to use the VASP code in this work and Claude Delmas for providing us X-ray diffraction data. X.R. thanks Dominique Guyomard and Yves Piffard for helpful discussions.

CM021254H